

Nanofibrillated lignocellulose-based superhydrophobic coating with antimicrobial performance

Mengting Ye

Qilu University of Technology (Shandong Academy of Sciences)

Shengdan Wang

Qilu University of Technology (Shandong Academy of Sciences)

Xingxiang Ji

Qilu University of Technology (Shandong Academy of Sciences)

Zhongjian Tian

Qilu University of Technology (Shandong Academy of Sciences)

Lin Dai

Tianjin University of Science and Technology

Chuanling Si (✉ sichli@tust.edu.cn)

Tianjin University of Science and Technology

Research Article

Keywords: Nanofibrillated lignocellulose, Superhydrophobicity, Coating, Antimicrobial

Posted Date: November 11th, 2022

DOI: <https://doi.org/10.21203/rs.3.rs-2219002/v1>

License: © ⓘ This work is licensed under a Creative Commons Attribution 4.0 International License.

[Read Full License](#)

Additional Declarations: No competing interests reported.

Version of Record: A version of this preprint was published at Advanced Composites and Hybrid Materials on December 31st, 2022. See the published version at <https://doi.org/10.1007/s42114-022-00602-3>.

Abstract

Superhydrophobic coatings have been widely developed to endue the materials with antibacterial, self-cleaning, antiseptic, and some other multi-functionalities. Fluorochemicals are the most commonly used superhydrophobic coatings, however, the released toxic substances from fluorinated polymers are a significant source of water pollution and even a threat to human health. With the increasingly great attention to the environment, it is imperative to exploit green and effective hydrophobic coatings. Here, a nanofibrillated lignocellulose-based multifunctional superhydrophobic coating (NMSC) was fabricated by using an efficient silylation process from cellulose, tetraethyl orthosilicate, and cetyl trimethoxysilane. Microscopic, chemical structural, and thermal properties analyses revealed that the NMSC has nano roughness, low surface energy, and good thermal stability. More importantly, the NMSC displayed an unprecedented hydrophobic and self-cleaning performance (water contact angle $\sim 165^\circ$). The NMSC superhydrophobic coating can realize long-term effective barriers to many fluids, including strong acid (pH = 1), strong alkali (pH = 13), alcohols, alkanes, esters, and some other organic solvents. Moreover, the NMSC also showed good antibacterial properties with *E. coli* and *S. aureus*. This work not only improved the high-value application of lignocellulose but also provides a good pathway for the development of ecological and sustainable multi-functional coatings.

1. Introduction

Superhydrophobic coatings have been widely developed to endue the materials with multi-functionality, including antibacterial[1], self-cleaning[2], antiseptic[3], and oil-water separation capacities[4]. Inspired by the natural interface structure of lotus leaves, the fabrication of micro/nano rough structures and reduction of surface free energy are the two main design approaches of superhydrophobic coatings[5]. Many studies have constructed the micro/nano rough structures from different raw materials (metals[6], alloys[7], ceramics[8]) by various fabrication methods[9], *e.g.* electrochemical etching[10], sol-gel processing[11], template syntheses[12], chemical vapor deposition[13], electrochemical method[14], layer-by-layer deposition[15]. However, most of these strategies are tedious, expensive, and resource intensive. On the other hand, the low surface energy contributes to the wetting transformation from hydrophilicity to superhydrophobicity[16]. Although, trifluoromethyl groups exhibit the lowest possible surface energy, the released toxic substance from fluorinated polymers are a significant source of water pollution and even a threat to human health. Therefore, it's very necessary to develop a facile and green approach to fabricate superhydrophobic coatings[17]-[18].

Lignocellulose is an economic and sustainable material, which is widely abundant in nature. Lignocellulose-based materials and their derivatives are sustainable, degradable, and environmentally friendly [19, 20]. Nanofibrillated lignocellulose (NFC) can be separated from lignocellulose using enzymatic pretreatment, oxidation pretreatment, or alkaline pretreatment followed by mechanical treatment. Owing to its nanoscale structure, modifiableness, biodegradability, and environmental friendliness[21–23], NFC has been extensively used in many fields such as antibacterial[24], anti-corrosion[25], UV protection[26], packaging[27], and gas barrier[28]. The surface of NFC contains a large

number of hydroxyl groups, which are easily modified by substances with low surface energy[29]. NFC has become one of the most promising green raw materials for the preparation of the fabrication of superhydrophobic coatings.

Surface grafting by a small amount of organic matter with low surface energy is an efficient and convenient way to form a superhydrophobic surface. Moreover, the surface roughness of NFC can be improved by organosilicon compounds, which have many good characteristics, including environmental protection, non-toxic, antioxidation, high-temperature and corrosion resistance. Herein, fluorine-free and environmentally benign NFC-based multifunctional superhydrophobic coatings (NMSC) were designed and fabricated by a facile coupling reaction of environmentally friendly ethyl orthosilicate and cetyl trimethoxysilane (Fig. 1a, b). Ethyl orthosilicate can be hydrolyzed into organosilicon by the breaking reaction of oxo-silicon bond catalyzed by ammonia water (Fig. 1c), which will provide a surface roughness for NFC. The hydrolyzation of hexadecyltrimethoxysilane into long-chain alkyl groups decreased the surface energy of NFC. The physicochemical, water-resisting, anticorrosive, and antibacterial properties of NMSC were systematically investigated.

2. Experimental Section

2.1 Materials

Bleached softwood kraft pulp (BSKP) was provided by Asia Pacific Senbo Paper Co., LTD (Shandong, China). Endoglucanase (Banzyme 2900) was obtained from UPM-kymmene Co., Ltd (Jiangsu, China). Ethyl orthosilicate reagents ($\text{Si}(\text{OCH}_2\text{CH}_3)_4$) and cetyltrimethoxysilane ($\text{CH}_3(\text{CH}_2)_{15}\text{Si}(\text{OCH}_3)_3$) were purchased from Aladdin (Shanghai, China). Absolute ethanol was obtained from Komeo Chemical Reagents Co, Ltd. (Tianjin, China). Tetraethyl orthosilicate and ammonia were purchased from Macklin (Shanghai, China). All of the chemicals are analytical grade and used as received.

2.2 Preparation of NFC

The BSKP was treated by a laboratory PFI mill (Hamjern Maskin; Hamar, Norway) according to TAPPIT 248 Laboratory beating of pulp (PFI mill method). Then, enzymatic pretreatment of BSKP was carried out according to previous work with some modifications[30]. Briefly, BSKP was suspended in enzyme-containing citrate acid-sodium citrate buffer (pH = 5.0, 9 mg/ g substrate). The mixture of samples was incubated at 50°C for 3 h. After enzymatic pretreatment, the slurry was centrifuged to separate the solid and liquid phases. The solid phases were diluted to 1 wt% and mechanically treated by a supermasscolloider (MKCA6-5J, Masuko Sangyo Co., Ltd., Japan). The obtained slurry at 0.5 wt% was further treated with an M-110EH-30 microfluidizer (Microfluidics, Newton, MA, USA) [31]. NFC was obtained after 25 passes through the microfluidizer at the slit pressure of 5000 psi.

2.3 Preparation of NMSC

NFC was washed with anhydrous ethanol to remove excess water. Tetraethyl orthosilicate (8 mL), ammonia (5 mL), and cetyl trimethoxysilane (4 mL) were added to a three-necked flask filled with 125 mL absolute ethanol under mechanical stirring at 250 rpm. Subsequently, the ethanol-washed NFC was added to the three-necked flask. The mixture was kept in Ultrasonic apparatus for 4 h and then washed thoroughly with anhydrous ethanol. The NMSC suspensions were obtained and stored at 4 °C for the following characterization.

2.4 Characterization

Scanning electron microscopy analysis (SEM). The surface microstructure and morphology of NFC and NMSC coating were examined using field emission scanning electron microscopy (FE-SEM, Hitachi Regulus 8220, Hitachi, Japan). All samples were oven-dried at room temperature and coated with a thin layer of gold before testing.

Contact angle analysis. Contact angles of the samples were measured using an LSA100 contact angle meter (LAUDA Scientific, Germany) at ambient temperature. For these measurements, 5 μ L of water was dropped on the substrate and allowed to stand for 5 s. All the samples were measured at least 3 times at different positions.

X-ray photoelectron spectrometer (XPS) and Fourier transform Infrared (FTIR). XPS and FTIR were conducted to determine the surface chemical structures of NFC and NMSC. The XPS data were performed on an ESCALAB 250Xi XPS with a monochromatic Al K α radiation. FTIR spectra were recorded using a Bruker instrument at ambient conditions by grinding the sample with KBr to prepare the pellet for analysis.

X-ray diffractometer (XRD). XRD detection was analyzed in the 2θ range from 5 to 40° on a Rigaku DMax-RB 91–0459 diffractometer with Cu K α radiation at a scan rate of 2°/min.

Thermogravimetric analysis (TGA). TGA measurements were acquired in a nitrogen atmosphere at a heating rate of 10 °C/ min by an STA446 F3 simultaneous thermal analyzer.

Corrosion resistant test. The cyclic method investigated the chemical stability of HBP under acid (pH = 1), alkali (pH = 13), and organic solvents (ethanol, chloroform, ethyl acetate). The corrosion resistance of NMSC was analyzed by combining the water-resisting properties of the coating samples in different environments for 100 min.

Bacteriostatic test. 0.1 mL bacteria suspension (10^{-4} CFU/mL) was inoculated onto a solid agar medium and dispersed with a coating rod. The agar plate with holes was opened by a perforator. The coating samples were placed in the hole of the agar solid medium and incubated under sterile conditions at 37 °C for 24 h.

3. Results And Discussion

3.1 Characterization of the coatings

Obtaining a superhydrophobic surface requires a specific rough structure and low surface energy. SEM image of NMSC shows many nanopapillae structures, which confirmed the successful coating of nano-silica on the surface of NFC (Fig. 1c). Compared to NFC, the water contact angle of NMSC increased from 42° to 169°.

The chemical structures of NMSC were investigated by FT-IR and XPS spectroscopy to verify the grafting reaction of organic silica with low surface energy long-chain alkyl groups. Figure 2a shows that the peak intensity at 3424.60 cm^{-1} corresponding to -OH stretching vibrations of NMSC decreased, which indicated the formation of Si-O-C. A noticeable enhancement of the absorption peaks at 2926.93 and 2857.64 cm^{-1} of NMSC is attributed to the symmetric and asymmetric stretching vibrations of long-chain alkyl groups (C-H) in silane coupling agents. Due to the bay oscillation of the C-H bond, a new absorption peak occurred at 1464.58 cm^{-1} [32]. Moreover, NMSC had a broad peak from 1000 to 1250 cm^{-1} , which could be due to the formation of siloxane bonds from the silane coupling agent and the surface hydroxyl groups of NFC, resulting in the overlap of the siloxane bond and the carbon-oxygen bond. The peaks observed in NMSC at 797.53 and 467.10 cm^{-1} were attributed to the Si-O bonds and the rocking vibration of the -CH₃ group, respectively[33].

The surface composition of NFC and NMSC was assessed by XPS. Compared with NFC, new peaks at 104 and 155 eV were observed in the XPS spectrum of NMSC, representing Si 2p and Si 2s, respectively (Fig. 2b). The high-resolution XPS spectra of carbon and silica on the NFC were showed in Fig. 2c. The C 1s envelope of the NFC is comprised of three components and is consistent with previous measurements of nanocellulose[34]. The envelope consisted of a dominant peak at 286.6 eV was attributed to the presence of C - O bonding. O-C = O binding energy peak at 287.9 eV corresponded to the acetal bond of NFC, and a peak at 284.8 eV, likely due to adventitious carbon. The intensity of the photoelectron transition increased at 284.8 eV (C-C or C-Si bonding) in NMSC was attributed to the introduction of Si - C carbon atoms (Fig. 2d). In contrast, the C - O and O - C-O peaks decreased in intensity as silanization[35]. Figure 2e confirmed the successful silylation of NFC.

XRD spectra of the NFC and NMSC samples demonstrate that the diffraction angles of the 002 and 101 lattice planes were changed obviously after grafting modification (Fig. 2f). The crystallization diffraction angle (2θ) appears new peak at around 23° owing to the silica-covering on the surface of NFC. These results also indicated the successful silylation of NFC.

Figure 3 shows the simultaneous thermal analysis of NFC and NMSC under the N₂ atmosphere. In the beginning, the weight loss was mainly caused by water evaporation. Due to the process of dehydration, the weight loss of NMSC was more than that of NFC. The hydroxyl groups were replaced by hydrophobic groups on the surface of NFC, and the surface water content was correspondingly reduced[36]. Furthermore, the thermal decomposition of NFC and NMSC happened from 100 to 400°C and 600°C, respectively. NFC had a significant decrease in maximum weight loss peak at 339.2°C with gradual heat

release and a residual mass (19.60%) after being heated to 800°C. Compared with NFC, NMSC had a higher maximum decomposition temperature (495.5°C) and residual mass ratio (51.57%), suggesting that the silylation of NFC significantly reinforced the thermostability of NMSC.

3.2 Self-cleaning property of NMSC

The NMSC showed high water repellency due to the synergistic effects of the nanoscale roughness and the low surface energy. Water droplets can exist stably on the surface of the glass with NMSC coating (Fig. 4a). Air pockets can also be clearly observed through the water beads. A water jet can be completely bounced off (Fig. 4b). When immersing the NMSC-coated glass in water, a mirror-like solid air layer formed on the interface. The above results demonstrated the good anti-fouling property of NMSC coating. The wettability of NMSC coating was monitored for 30 days (Fig. 4b). The average value of contact angles was 165° ($\pm 4^\circ$), which demonstrates its good stability of water resistance. The self-cleaning property of coating had been active in the field of people[37]. As shown in Fig. 5a, NMSC coating can effectively prevent MnO₂ sewage. Moreover, the heavily scratched NMSC coating still exhibited superhydrophobic and self-cleaning properties (Fig. 5b).

3.3 The corrosion resistance of NMSC

The fluidity of water droplets on the surface of NMSC coating can reveal its corrosion resistance. As shown in Fig. 6, after immersing in HCl (pH 1) and NaOH (pH 13) solution for 100 min and multiple treatments, the NMSC coating kept good water-resistance performance. The static CA of NMSC coating after cycle treatments is shown in Fig. 6c. The static contact angles of NMSC were above 155° throughout the whole process of acid/alkali treatments, which revealed its excellent acid and alkali resistance. These phenomena could be benefited from the rough micro-/nano-structure and low surface energy that trap air and form an air cushion to reduce contact with acids and bases effectively.

The corrosion of coatings from organic solvents can not be ignored. Superhydrophobic surfaces are easily damaged by wetting with low surface tension solutions[38]. Here, ethanol, chloroform, and ethyl acetate were further used to evaluate the organic solvent corrosion resistance. The NMSC coating samples were immersed in different organic solvents for 100 min, and then tested by evaluated by contact angle tests. The little change in the contact angle values before and after treatments suggested that NMSC coating also has strong corrosion resistance against organic solvents. It should be noted that the superhydrophobic property of NMSC was briefly lost after being soaked in different organic solvents. Nevertheless, the superhydrophobic property of NMSC was not damaged and was recovered after organic solvent evaporation (Fig. 7b-d). It might be due to the hydrogen bonding force between a few unreacted hydroxyl groups, which promotes the specific self-healing property of NMSC in organic solvents.

3.4 Antibacterial properties of NMSC

Bacteria resistance could also be important to coatings. The inhibitory zone method was measured to evaluate the antibacterial properties of NMSC against gram-positive (*S. aureus*) and gram-negative (*E. coli*) bacteria (Fig. 8). The better antibacterial performance of NMSC might be attributed to its

hydrophobic surface which readily penetrated the phospholipid bilayer of bacteria and disrupted the bacterial cell membrane, resulting a severe loss of cell structure integrity and leakage of cytoplasmic content and the lysis of the bacterial cell[39]. In addition, *E. coli* was more sensitive to NMSC than *S. aureus* at the same liquid ratios, which could be due to the hydrophilic and hydrophobic outer membrane of gram-negative and gram-positive bacteria, respectively[40].

4. Conclusion

In summary, a simple, green, and effective nanocellulose-based multifunctional superhydrophobic coatings (NMSC) was designed and synthesized by using a silylation technology. The NMSC coating has good superhydrophobic, self-cleaning properties, corrosion resistance, and antibacterial properties. The NMSC superhydrophobic coating can realize long-term effective barriers to acid, alkali, alcohols, and organic solvents. Moreover, the NMSC also showed good antibacterial properties with *E. coli* and *S. aureus*. Due to its eco-friendly, superhydrophobic, and antibacterial properties, the NMSC has extensive application prospects in many fields, such as food packaging, oil-water separation, and medicine.

Declarations

Funding

This work was supported by the National Natural Science Foundation of China (Grant No. 31870566), Natural Science Foundation of Shandong Province of China (Grant No. ZR2020QE097), Jinan Innovation Team (Grant No. 2021GXRC023), and Taishan Scholars Program.

Conflict of interest

The authors declare no competing interests.

Authorship contribution statement

Xingxiang Ji supervised the project. Mengting Ye and Xingxiang Ji designed the experiments. Mengting Ye performed the experiments. All authors discussed experiments and results. Mengting Ye wrote the manuscript. All authors have given approval to the final version of the manuscript.

References

1. Razavi SMR, Oh J, Haasch RT, Kim K, Masoomi M, Bagheri R, Slauch JM, Miljkovic N (2019) Environment-Friendly Antibiofouling Superhydrophobic Coatings. *ACS Sustainable Chemistry & Engineering* 7 (17):14509-14520. doi:10.1021/acssuschemeng.9b02025
2. Chen S, Song Y, Xu F (2018) Highly Transparent and Hazy Cellulose Nanopaper Simultaneously with a Self-Cleaning Superhydrophobic Surface. *ACS Sustainable Chemistry & Engineering* 6 (4):5173-5181. doi:10.1021/acssuschemeng.7b04814

3. Yang X, Tian L, Wang W, Fan Y, Sun J, Zhao J, Ren L (2020) Bio-inspired Superhydrophobic Self-healing Surfaces with Synergistic Anticorrosion Performance. *Journal of Bionic Engineering* 17 (6):1196-1208. doi:10.1007/s42235-020-0094-4
4. Kang L, Li J, Zeng J, Gao W, Xu J, Cheng Z, Chen K, Wang B (2019) A water solvent-assisted condensation polymerization strategy of superhydrophobic lignocellulosic fibers for efficient oil/water separation. *Journal of Materials Chemistry A* 7 (27):16447-16457. doi:10.1039/c9ta04815d
5. Wen L, Tian Y, Jiang L (2015) Bioinspired super-wettability from fundamental research to practical applications. *Angew Chem Int Ed Engl* 54 (11):3387-3399. doi:10.1002/anie.201409911
6. Mousavi SMA, Pitchumani R (2021) A study of corrosion on electrodeposited superhydrophobic copper surfaces. *Corrosion Science* 186. doi:10.1016/j.corsci.2021.109420
7. Chobaomsup V, Metzner M, Boonyongmaneerat Y (2020) Superhydrophobic surface modification for corrosion protection of metals and alloys. *Journal of Coatings Technology and Research* 17 (3):583-595. doi:10.1007/s11998-020-00327-2
8. Usman J, Othman MHD, Ismail AF, Rahman MA, Jaafar J, Raji YO, Gbadamosi AO, El Badawy TH, Said KAM (2021) An overview of superhydrophobic ceramic membrane surface modification for oil-water separation. *Journal of Materials Research and Technology* 12:643-667. doi:10.1016/j.jmrt.2021.02.068
9. Yan YY, Gao N, Barthlott W (2011) Mimicking natural superhydrophobic surfaces and grasping the wetting process: a review on recent progress in preparing superhydrophobic surfaces. *Adv Colloid Interface Sci* 169 (2):80-105. doi:10.1016/j.cis.2011.08.005
10. Lu Y, Song J, Liu X, Xu W, Xing Y, Wei Z (2012) Preparation of Superoleophobic and Superhydrophobic Titanium Surfaces via an Environmentally Friendly Electrochemical Etching Method. *ACS Sustainable Chemistry & Engineering* 1 (1):102-109. doi:10.1021/sc3000527
11. Wu X, Fu Q, Kumar D, Ho JWC, Kanhere P, Zhou H, Chen Z (2016) Mechanically robust superhydrophobic and superoleophobic coatings derived by sol-gel method. *Materials & Design* 89:1302-1309. doi:10.1016/j.matdes.2015.10.053
12. Lin, Feng, Dr., Shuhong, Li, Dr., Huanjun, Li, Dr., Jin (2002) Super-Hydrophobic Surface of Aligned Polyacrylonitrile Nanofibers. *Angewandte Chemie*
13. Geyer FL, Ueda E, Liebel U, Grau N, Levkin PA (2011) Superhydrophobic-superhydrophilic micropatterning: towards genome-on-a-chip cell microarrays. *Angew Chem Int Ed Engl* 50 (36):8424-8427. doi:10.1002/anie.201102545
14. Nicolas M, Guittard F, G ribaldi S (2006) Synthesis of Stable Super Water- and Oil-Repellent Polythiophene Films. *Angewandte Chemie* 118 (14):2309-2312. doi:10.1002/ange.200503892
15. Li Y, Liu F, Sun J (2009) A facile layer-by-layer deposition process for the fabrication of highly transparent superhydrophobic coatings. *Chem Commun (Camb)* (19):2730-2732. doi:10.1039/b900804g
16. Kang L, Wang B, Zeng J, Cheng Z, Li J, Xu J, Gao W, Chen K (2020) Degradable dual superlyophobic lignocellulosic fibers for high-efficiency oil/water separation. *Green Chemistry* 22 (2):504-512.

doi:10.1039/c9gc03861b

17. Ellinas K, Dimitrakellis P, Sarkiris P, Gogolides E (2021) A Review of Fabrication Methods, Properties and Applications of Superhydrophobic Metals. *Processes* 9 (4). doi:10.3390/pr9040666
18. Wu W, Wang X, Liu X, Zhou F (2009) Spray-coated fluorine-free superhydrophobic coatings with easy repairability and applicability. *ACS Appl Mater Interfaces* 1 (8):1656-1661. doi:10.1021/am900136k
19. Dai L, Lu J, Kong F, Liu K, Wei H, Si C (2019) Reversible photo-controlled release of bovine serum albumin by azobenzene-containing cellulose nanofibrils-based hydrogel. *Advanced Composites and Hybrid Materials* 2 (3):462-470. doi:10.1007/s42114-019-00112-9
20. Fatima A, Yasir S, Ul-Islam M, Kamal T, Ahmad MW, Abbas Y, Manan S, Ullah MW, Yang G (2021) Ex situ development and characterization of green antibacterial bacterial cellulose-based composites for potential biomedical applications. *Advanced Composites and Hybrid Materials*. doi:10.1007/s42114-021-00369-z
21. Cherian RM, Tharayil A, Varghese RT, Antony T, Kargarzadeh H, Chirayil CJ, Thomas S (2022) A review on the emerging applications of nano-cellulose as advanced coatings. *Carbohydr Polym* 282:119123. doi:10.1016/j.carbpol.2022.119123
22. Xie Z, Tian Z, Liu S, Ma H, Ji X-X, Si C (2022) Effects of different amounts of cellulase on the microstructure and soluble substances of cotton stalk bark. *Advanced Composites and Hybrid Materials*. doi:10.1007/s42114-021-00400-3
23. Ran F, Li C, Hao Z, Zhang X, Dai L, Si C, Shen Z, Qiu Z, Wang J (2022) Combined bactericidal process of lignin and silver in a hybrid nanoparticle on E. coli. *Adv Compos Hybrid Mater*:1-11. doi:10.1007/s42114-022-00460-z
24. Li J, Cha R, Mou K, Zhao X, Long K, Luo H, Zhou F, Jiang X (2018) Nanocellulose-Based Antibacterial Materials. *Adv Healthc Mater* 7 (20):e1800334. doi:10.1002/adhm.201800334
25. He Y, Li G, Hwang K-H, Boluk Y, Claesson PM (2021) Nano-scale mechanical and wear properties of a corrosion protective coating reinforced by cellulose nanocrystals – Initiation of coating degradation. *Applied Surface Science* 537. doi:10.1016/j.apsusc.2020.147789
26. Joram Mendoza D, Mouterde LMM, Browne C, Singh Raghuwanshi V, Simon GP, Garnier G, Allais F (2020) Grafting Nature-Inspired and Bio-Based Phenolic Esters onto Cellulose Nanocrystals Gives Biomaterials with Photostable Anti-UV Properties. *ChemSusChem* 13 (24):6552-6561. doi:10.1002/cssc.202002017
27. Yu Z, Dhital R, Wang W, Sun L, Zeng W, Mustapha A, Lin M (2019) Development of multifunctional nanocomposites containing cellulose nanofibrils and soy proteins as food packaging materials. *Food Packaging and Shelf Life* 21. doi:10.1016/j.fpsl.2019.100366
28. Fotie G, Rampazzo R, Ortenzi MA, Checchia S, Fessas D, Piergiovanni L (2017) The Effect of Moisture on Cellulose Nanocrystals Intended as a High Gas Barrier Coating on Flexible Packaging Materials. *Polymers (Basel)* 9 (9). doi:10.3390/polym9090415
29. Hu F, Zeng J, Cheng Z, Wang X, Wang B, Zeng Z, Chen K (2021) Cellulose nanofibrils (CNFs) produced by different mechanical methods to improve mechanical properties of recycled paper.

- Carbohydr Polym 254:117474. doi:10.1016/j.carbpol.2020.117474
30. Wang S, Gao W, Chen K, Xiang Z, Zeng J, Wang B, Xu J (2018) Deconstruction of cellulosic fibers to fibrils based on enzymatic pretreatment. *Bioresour Technol* 267:426-430. doi:10.1016/j.biortech.2018.07.067
 31. Yang G, Ma G, He M, Ji X, Li W, Youn HJ, Lee HL, Chen J (2021) Comparison of Effects of Sodium Chloride and Potassium Chloride on Spray Drying and Redispersion of Cellulose Nanofibrils Suspension. *Nanomaterials (Basel)* 11 (2). doi:10.3390/nano11020439
 32. Li J, Xu C, Zhang Y, Wang R, Zha F, She H (2016) Robust superhydrophobic attapulgite coated polyurethane sponge for efficient immiscible oil/water mixture and emulsion separation. *Journal of Materials Chemistry A* 4 (40):15546-15553. doi:10.1039/c6ta07535e
 33. Zhang K, Yang X, Zhu N, Wang Z-C, Yan H (2017) Environmentally benign paints for superhydrophobic coatings. *Colloid and Polymer Science* 295 (4):709-714. doi:10.1007/s00396-017-4053-5
 34. Wu X, Wu L, Tan J, Chen GY, Owens G, Xu H (2018) Evaporation above a bulk water surface using an oil lamp inspired highly efficient solar-steam generation strategy. *Journal of Materials Chemistry A* 6 (26):12267-12274. doi:10.1039/c8ta03280g
 35. Lakshmi RV, Bera P, Anandan C, Basu BJ (2014) Effect of the size of silica nanoparticles on wettability and surface chemistry of sol-gel superhydrophobic and oleophobic nanocomposite coatings. *Applied Surface Science* 320:780-786. doi:10.1016/j.apsusc.2014.09.150
 36. You X, Hu Q, Hu X, Chen H, Yang W, Zhang X (2019) An Effective, Economical and Ultra-Fast Method for Hydrophobic Modification of NCC Using Poly(Methylhydrogen)Siloxane. *Polymers (Basel)* 11 (6). doi:10.3390/polym11060963
 37. Kang L, Shi L, Zeng Q, Liao B, Wang B, Guo X (2021) Melamine resin-coated lignocellulose fibers with robust superhydrophobicity for highly effective oil/water separation. *Separation and Purification Technology* 279. doi:10.1016/j.seppur.2021.119737
 38. Pashinin AS (2016) Interaction of superhydrophobic materials with aqueous solutions and organic solvents. *Russian Chemical Bulletin* 65 (1):98–102
 39. Manukumar HM, Umesha S (2017) Photocrosslinker technology: An antimicrobial efficacy of cinnamaldehyde cross-linked low-density polyethylene (Cin-C-LDPE) as a novel food wrapper. *Food Res Int* 102:144-155. doi:10.1016/j.foodres.2017.09.095
 40. Liu F, Turker Saricaoglu F, Avena-Bustillos RJ, Bridges DF, Takeoka GR, Wu VCH, Chiou BS, Wood DF, McHugh TH, Zhong F (2018) Preparation of Fish Skin Gelatin-Based Nanofibers Incorporating Cinnamaldehyde by Solution Blow Spinning. *Int J Mol Sci* 19 (2). doi:10.3390/ijms19020618

Figures

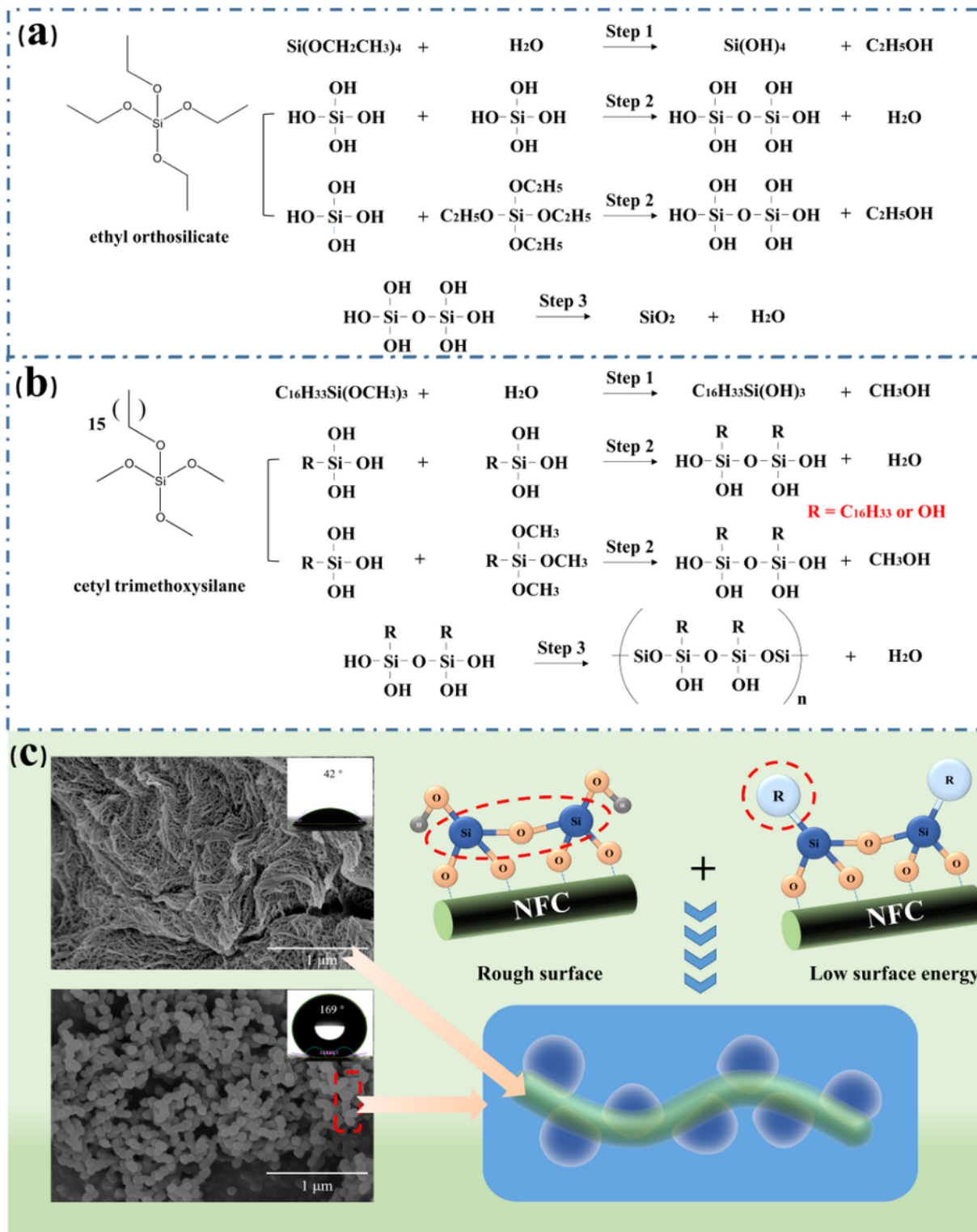


Figure 1

(a) Hydrolysis reaction mechanism of ethyl orthosilicate on the surface of NFC. (b) Hydrolysis mechanism of cetyl trimethoxysilane on the surface of NFC. (c) SEM and water CA image of NMCS and NFC, and Schematic diagram of NMCS formation.

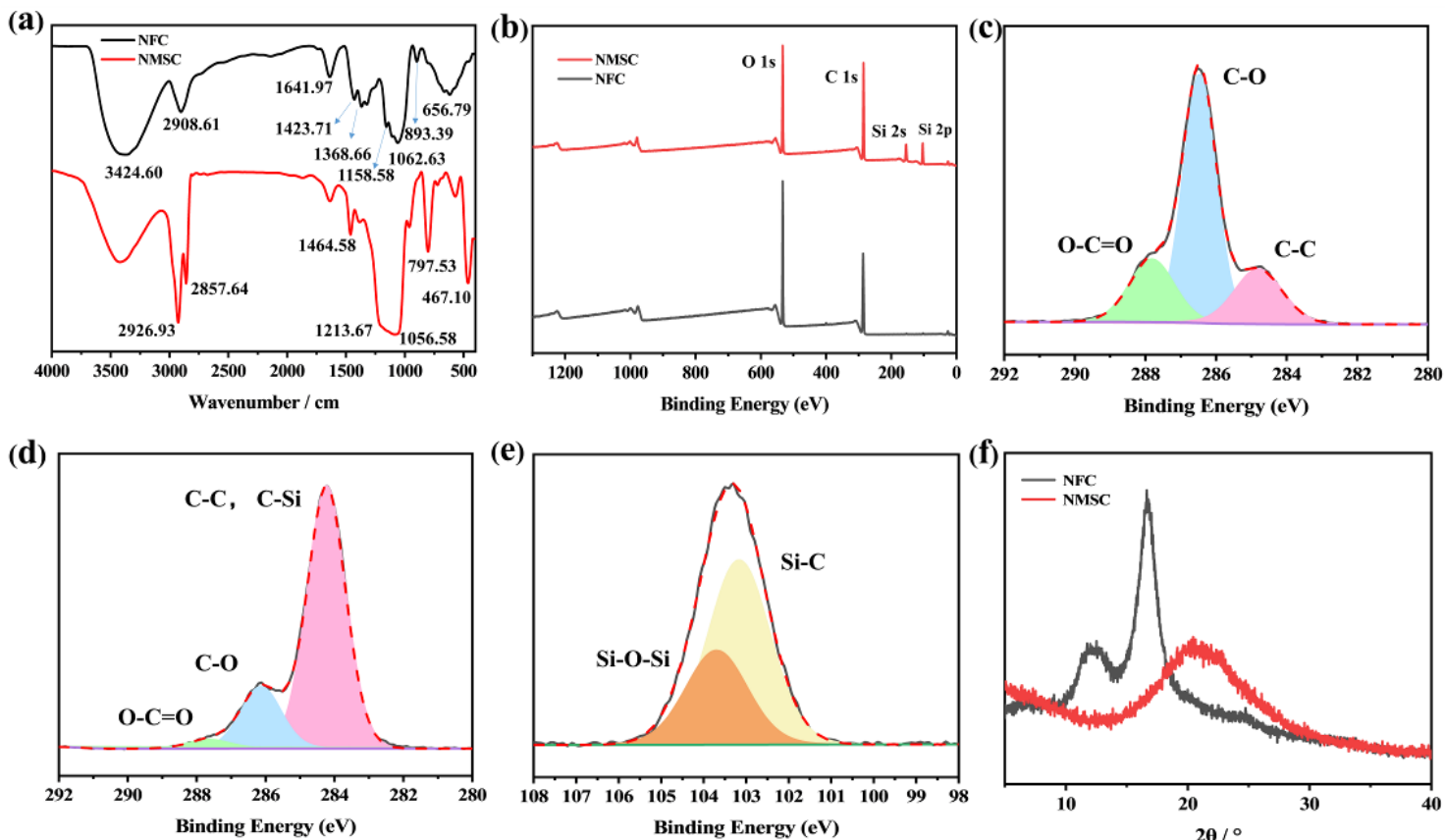


Figure 2

(a) FT-IR spectra of the NFC and the NMSC. (b) XPS spectrum of NFC and NMSC. (c and d) C 1s of NFC and NMSC. (e) Si 2p of NMSC. (f) XRD patterns of NFC and NMSC.

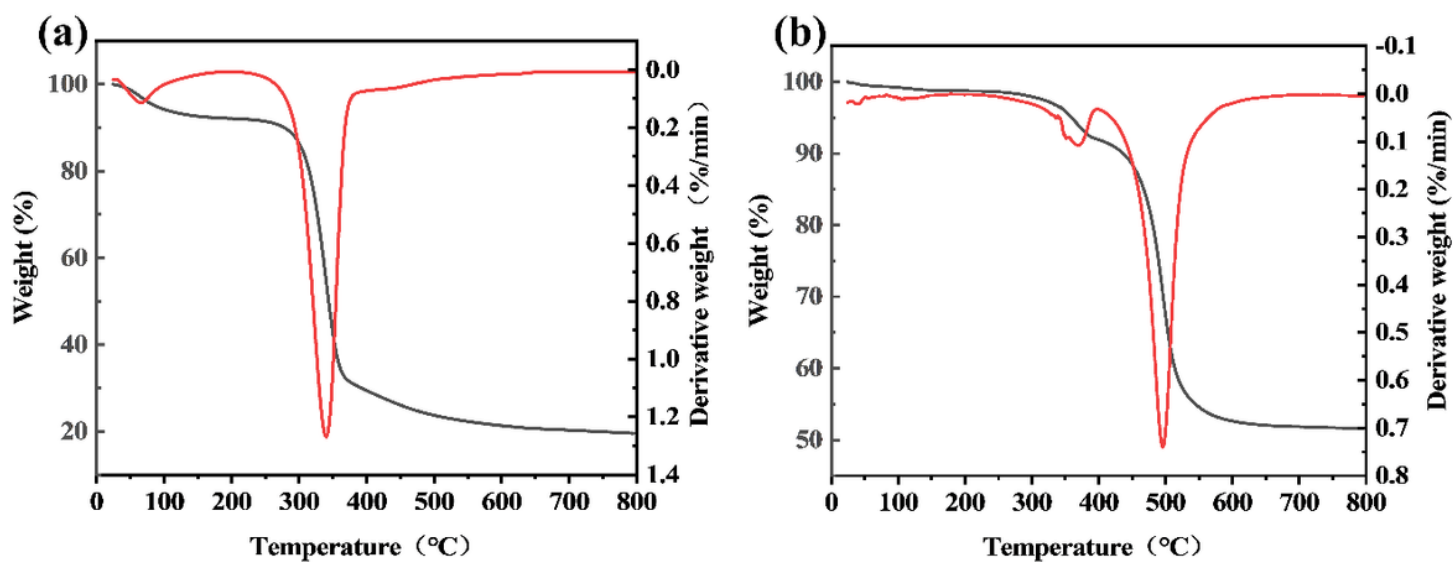


Figure 3

Thermogravimetric and derivative curves of NFC (a) and NMSC (b).

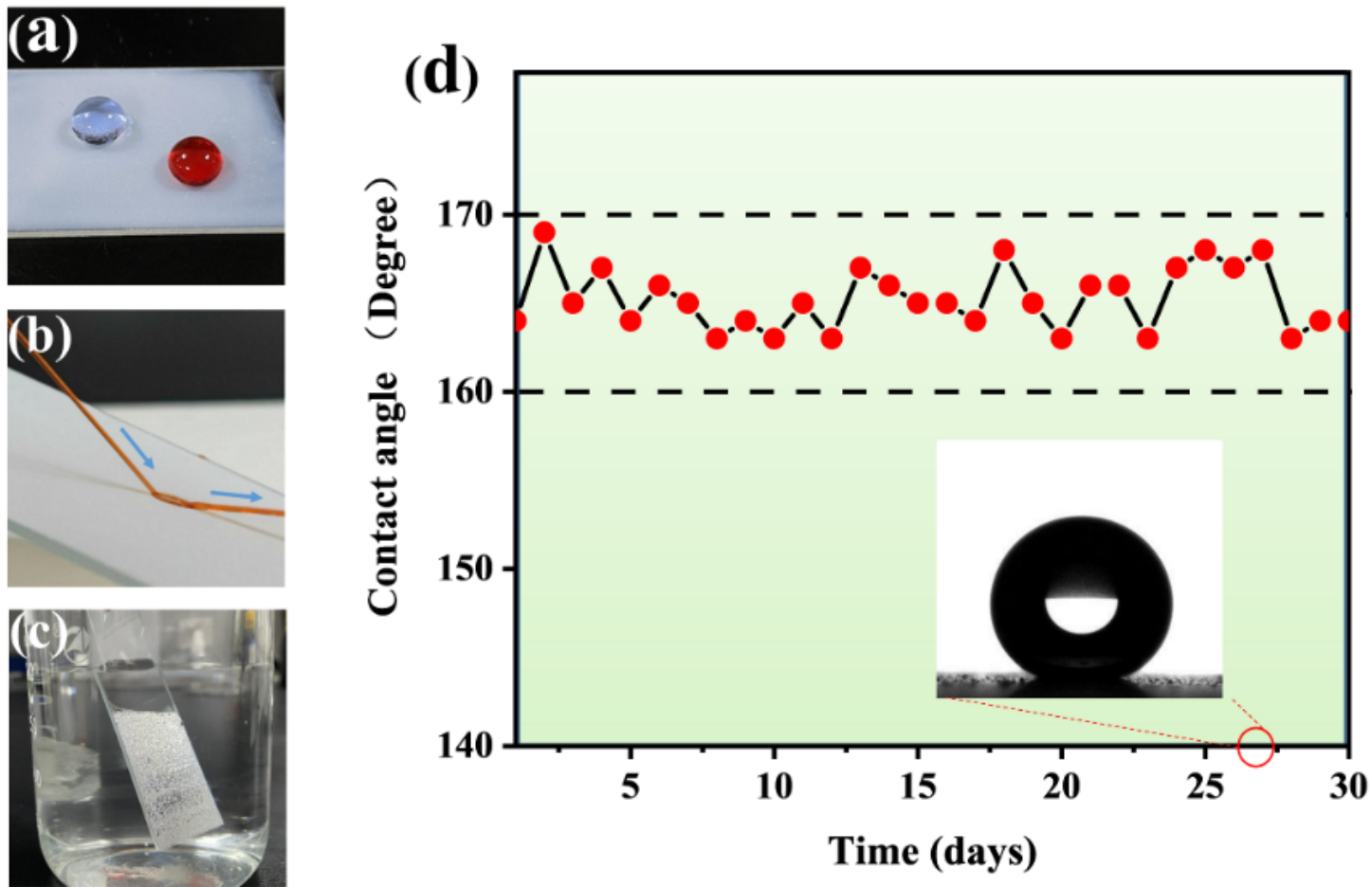


Figure 4

(a-c) Superhydrophobic effect of NMSC. (d) The monitoring of contact angles of the coatings in water.

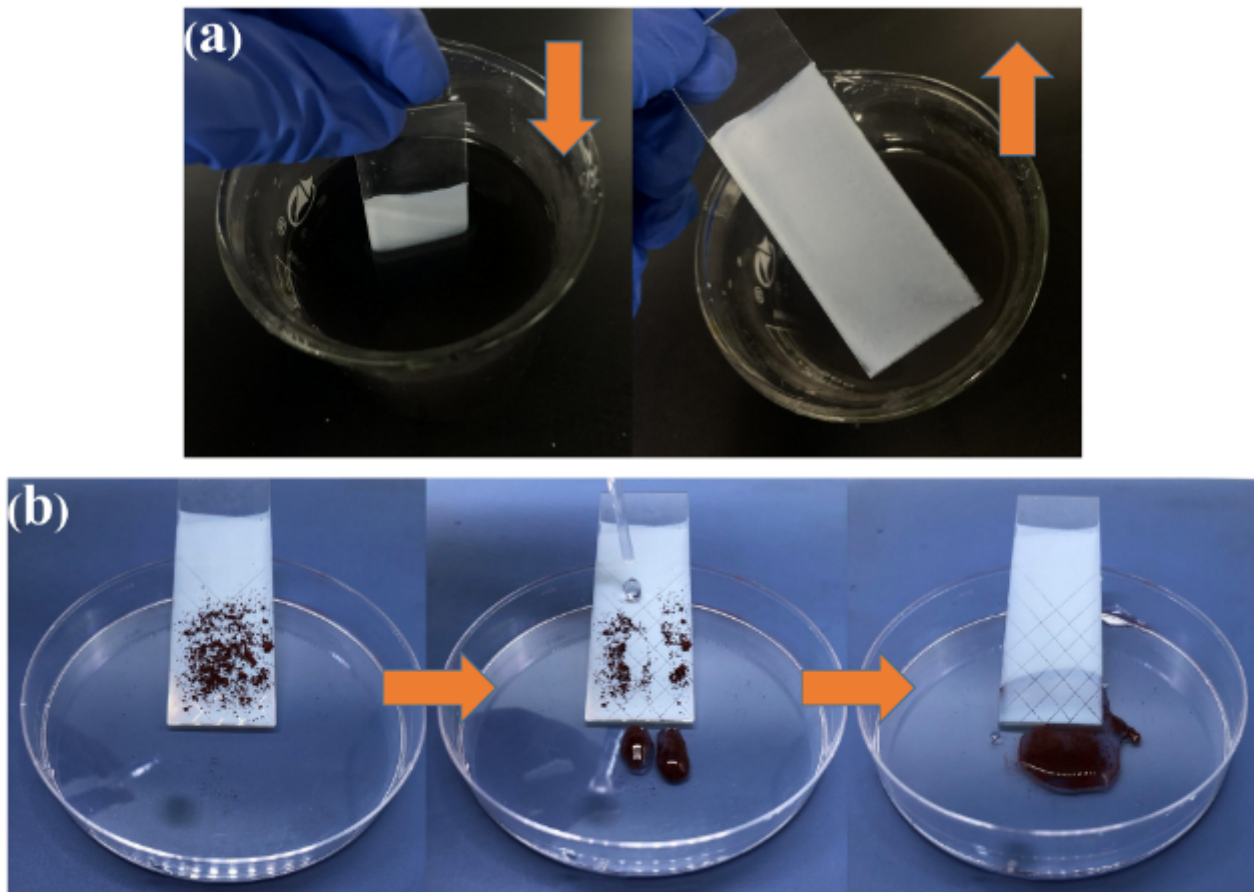


Figure 5

(a) Anti-polluting of NMSC coating after immersing in MnO_2 dyed water. (b) Self-cleaning property of heavily scratched NMSC coating.

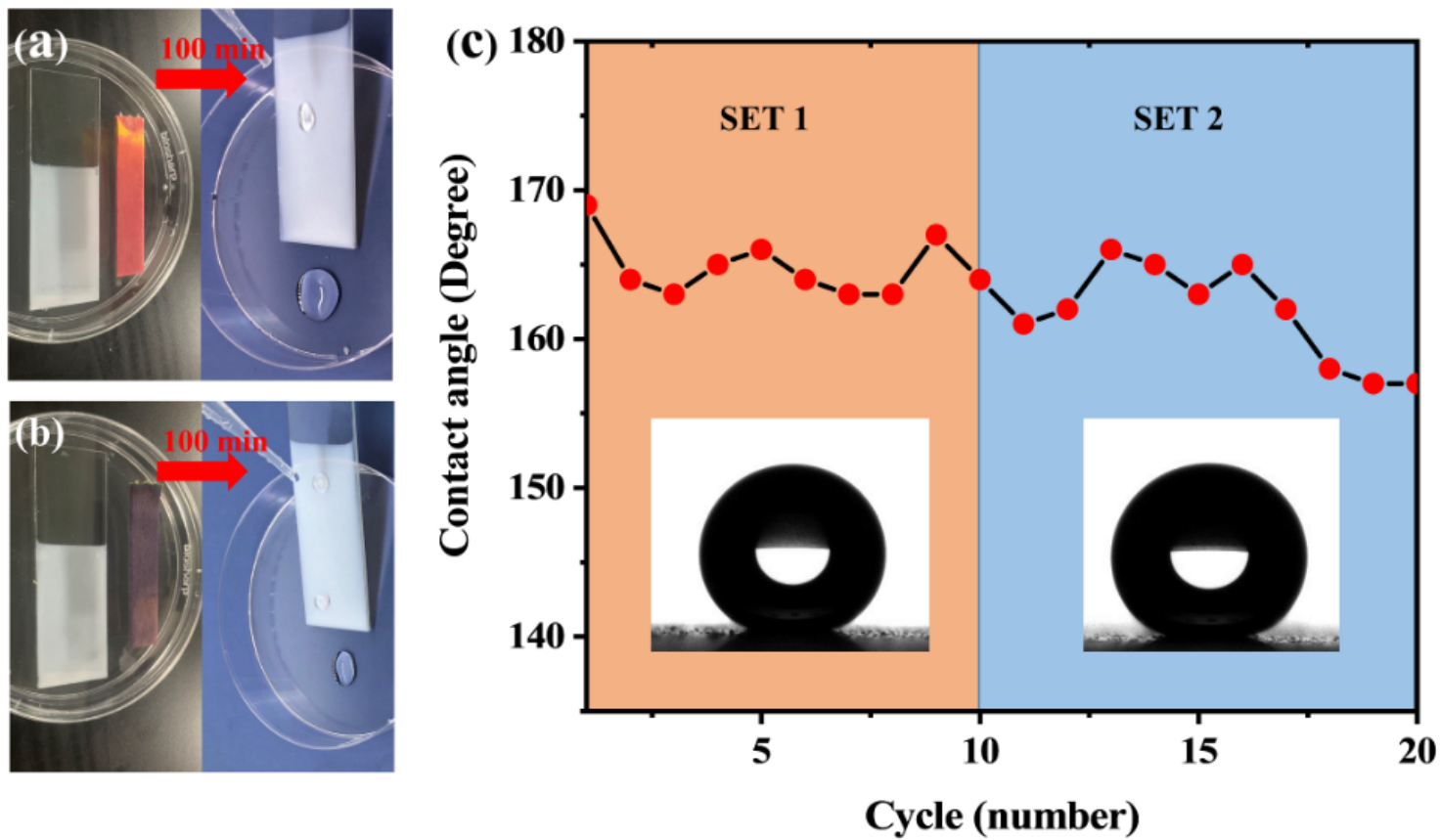


Figure 6

Water-resistance of NMSC coating after immersing in HCl (pH 1, a) and NaOH (pH 13, b) solution for 100 min. (c) Water-resistance of NMSC coating after multiple treatments by acid (Set 1) and alkali (Set 2).

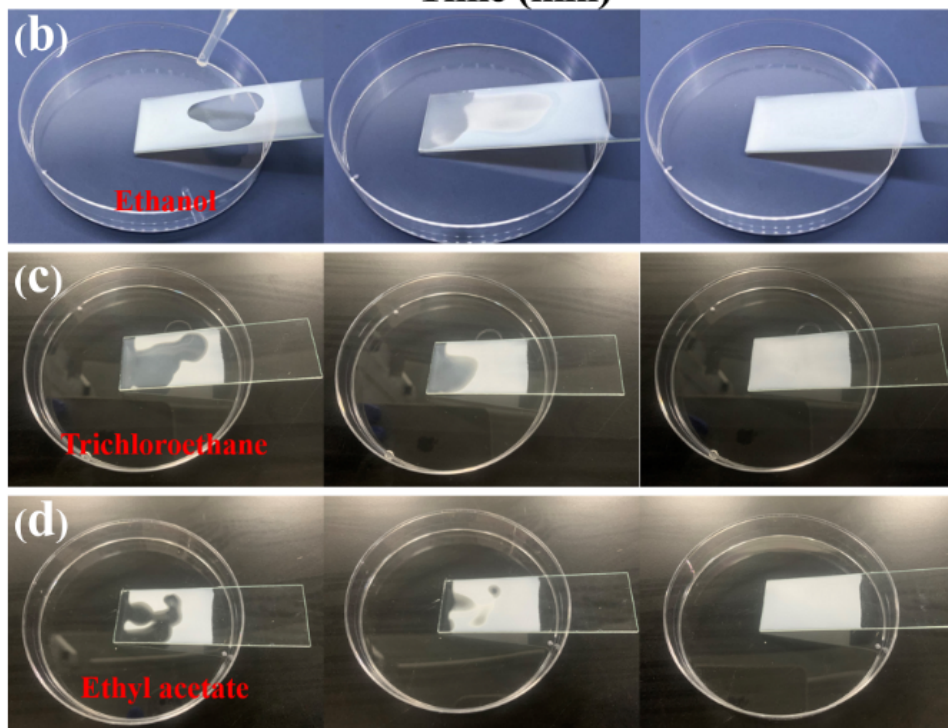
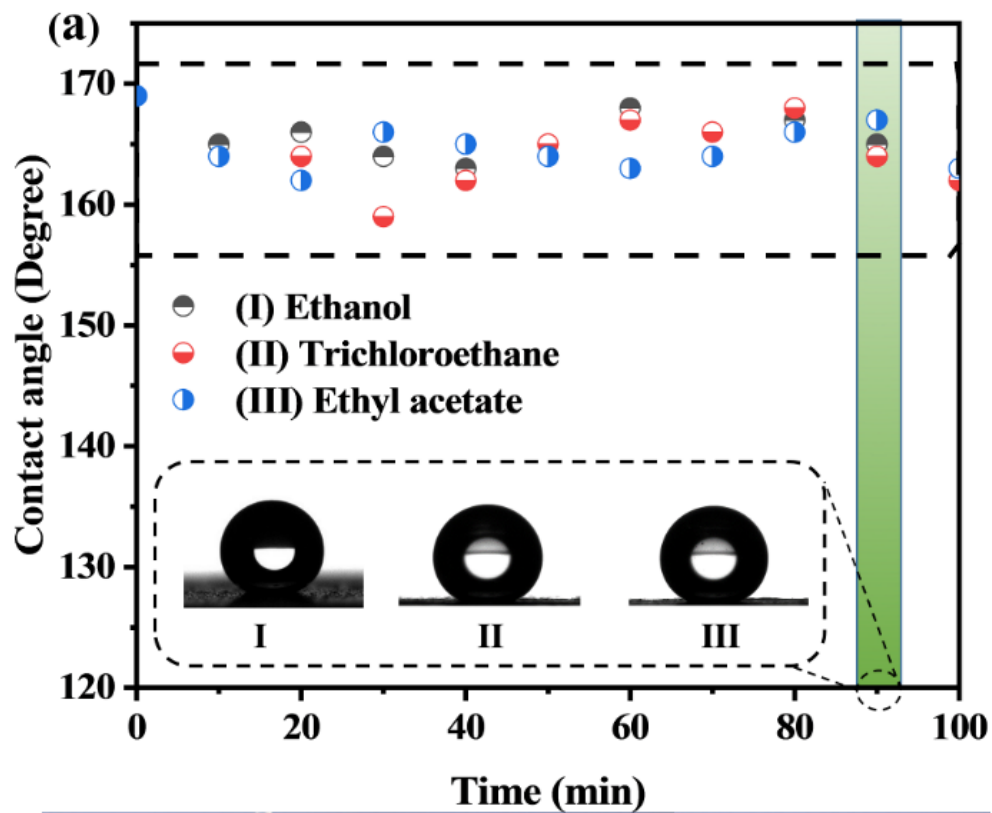


Figure 7

(a) The CA of NMSC in different organic solvents immersion tested several times in succession (inset photograph, i.e., the 9th test, immersion for 90 min). (b-d) Self-recovery of NMSC under different organic solvents.

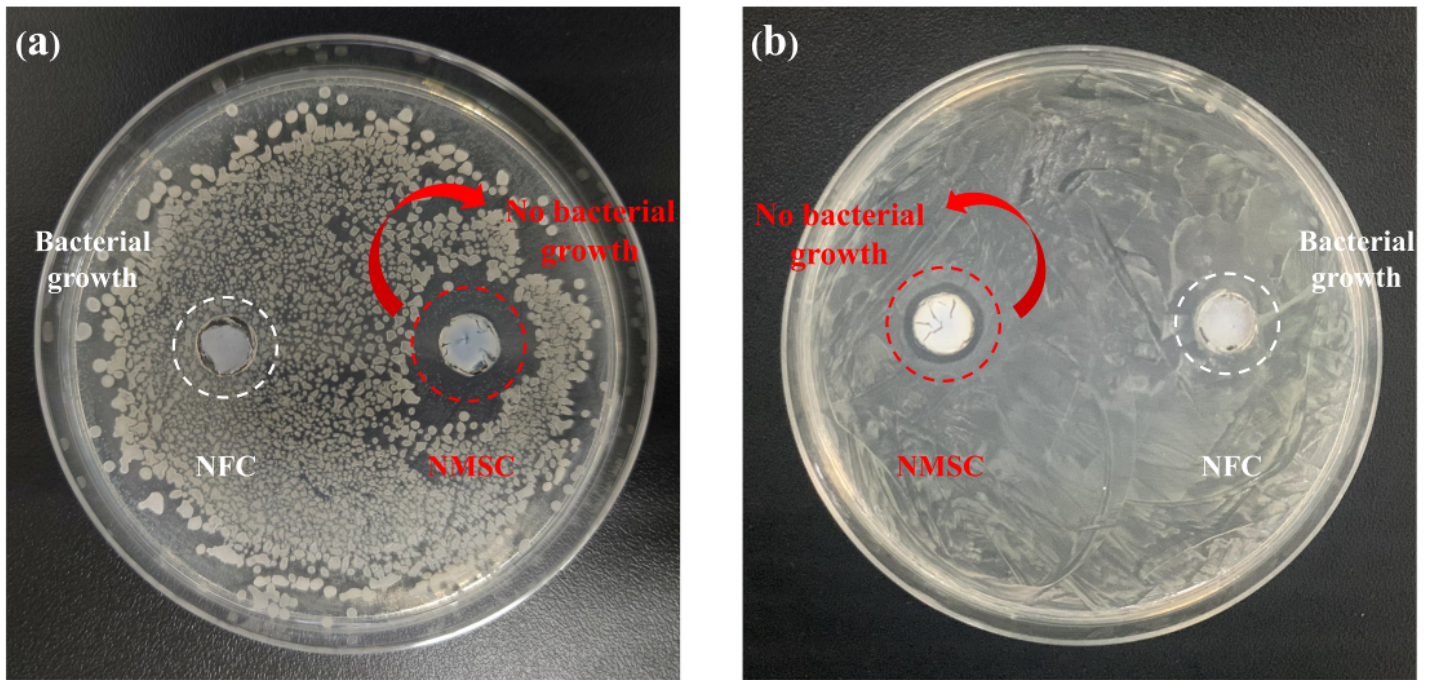


Figure 8

Antibacterial properties, (a) *E. coli* and (b) *S. aureus*.

Supplementary Files

This is a list of supplementary files associated with this preprint. Click to download.

- [GraphicalAbstract.png](#)